ELSEVIER

Biochimica et Biophysica Acta 1565 (2002) 294–307

BIOCHIMICA ET BIOPHYSICA ACTA
BBA

www.bba-direct.com

Review

Potassium channels: structures, models, simulations

Mark S.P. Sansom[a,*], Indira H. Shrivastava[b], Joanne N. Bright[a], John Tate[c], Charlotte E. Capener[a], Philip C. Biggin[a]

[a] *Laboratory of Molecular Biophysics, Department of Biochemistry, The University of Oxford, The Rex Richards Building, South Parks Road, Oxford OX1 3QU, UK*
[b] *LECB, NCI, MSC 5677, Bethesda, MD 20892, USA*
[c] *EMBL Outstation-Hinxton, European Bioinformatics Institute, Wellcome Trust Genome Campus, Hinxton Hall, Cambridge CB10 1SD, UK*

Received 16 January 2002; received in revised form 27 June 2002; accepted 2 July 2002

Abstract

Potassium channels have been studied intensively in terms of the relationship between molecular structure and physiological function. They provide an opportunity to integrate structural and computational studies in order to arrive at an atomic resolution description of mechanism. We review recent progress in K channel structural studies, focussing on the bacterial channel KcsA. Structural studies can be extended via use of computational (i.e. molecular simulation) approaches in order to provide a perspective on aspects of channel function such as permeation, selectivity, block and gating. Results from molecular dynamics simulations are shown to be in good agreement with recent structural studies of KcsA in terms of the interactions of K^+ ions with binding sites within the selectivity filter of the channel, and in revealing the importance of filter flexibility in channel function. We discuss how the KcsA structure may be used as a template for developing structural models of other families of K channels. Progress in this area is explored via two examples: inward rectifier (Kir) and voltage-gated (Kv) potassium channels. A brief account of structural studies of ancillary domains and subunits of K channels is provided.

Keywords: Potassium channel; Simulation; Molecular structure

1. Introduction to K channels

Ion channels are integral membrane proteins that span lipid bilayers to form a central pore through which selected ions can pass at near diffusion-limited rates (ca. 10^7 ions channel^{-1} s^{-1}) They govern the electrical properties of the membranes of excitable cells such as neurones [1]. In addition, ion channels play a more general role in membrane physiology and are found in a wide range of organisms from viruses and bacteria to plants and mammals. Potassium channels are a large family of ion channels that share a common property of selectivity for K^+ over Na^+ ions. As a result of advances in structural and computational biology, K channels provide a paradigm for the study of ion channels (and for membrane transport proteins in general).

It is useful to recall the level at which the molecular properties of K channels were understood in advance of determination of an X-ray structure. Analysis of K channel sequences had enabled design of experiments to explore relationships between sequence motifs and various aspects of physiological function [2–5]. In particular, it was shown that the selectivity of K channels for potassium ions was associated with a conserved sequence motif TVGYG located in a re-entrant loop present in between two predicted transmembrane (TM) α-helices. This sequence motif, conserved across all K channels, was proposed to correspond to the *selectivity filter* of the pore-forming region of the channel protein. K channels are tetrameric and thus four copies of the filter motif come together to form the pore (Fig. 1). More detailed molecular physiological studies assigned functional roles (e.g. susceptibility to channel block; control of channel gating) to other regions of voltage-gated potassium (Kv) channels. These studies enabled formulation of some basic questions to be answered by structural and computational studies. For example, one may ask what are the atomic resolution events underlying phenomena such as ion permeation, ion selectivity, channel block, and channel gating?

* Corresponding author. Tel.: +44-1865-275371; fax: +44-1865-275182.
E-mail address: mark@biop.ox.ac.uk (M.S.P. Sansom).

0005-2736/02/$ - see front matter
PII: S0005-2736(02)00576-X

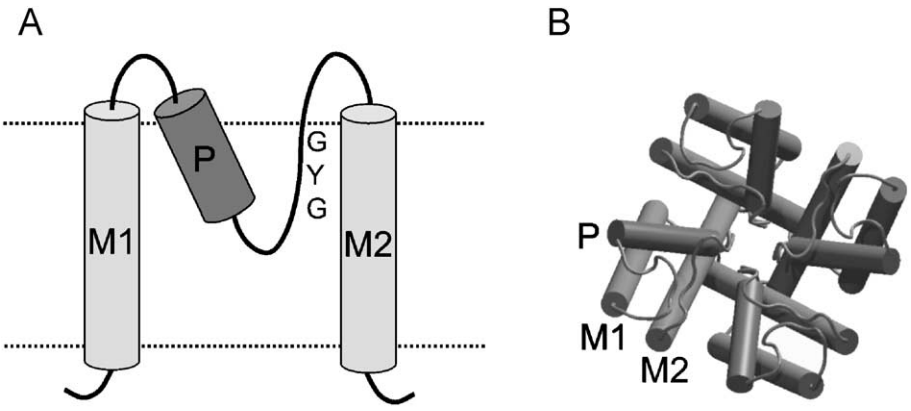

Fig. 1. Potassium channel topology. (A) The transmembrane topology of the simple bacterial K channel, KcsA. Each subunit contains two transmembrane helices (M1 and M2) with an intervening loop made up of a short helix (P) and the selectivity filter that contains the GYG sequence motif. The location of the lipid bilayer is indicated by the horizontal dotted lines. (B) View down a tetrameric K channel bundle looking from the extracellular mouth into the central pore. The M1, P and M2 helices are labelled.

There are several families of K channels in animals [6], including: (i) Kv channels (activated by a change in transmembrane voltage); (ii) inward rectifier channels (Kirs), which have a higher conductance for K^+ ions moving into the cell than outwards and are often regulated by intracellular factors; and (iii) TWIK and related channels, which contain two copies of the selectivity filter motif in one polypeptide chain, two chains coming together to form the intact channel. Our knowledge of K channel structure is derived mainly from a simple bacterial channel, KcsA from *Streptomyces lividans* [7], which resembles the Kirs in its TM topology. Although (see below) Kv channels have a more complex TM topology than KcsA, KcsA resembles Kv channels closely in terms of ion permeation, selectivity and block [8,9]. The main differences between KcsA and Kv channels are in their gating mechanisms: KcsA is opened by a lowering of pH [10,11] in contrast to Kv channels, which are activated by cell membrane depolarisation.

In this review, we describe the structure of KcsA, and its functional implications. In particular, we explore whether or not our understanding of K channel physiology approaches atomic resolution, i.e. the extent to which we are able to explain single channel physiology in terms of atomic resolution structure. We also explore how insights gained from studies of KcsA may be extended to other types of K channels. The overall emphasis of our discussion is on how integration of experimental and computational structural approaches may be used to reveal the physical basis of physiological function. Some other recent reviews have focussed on either structural [12–14] or computational [15–17] aspects.

2. The structure of KcsA: from fold to function

There are a number of structures available for KcsA (see Table 1). The original X-ray structure at 3.2 Å [18] was solved in the presence of 150 mM K^+ ions at pH 7.5. More recently, structures have been solved using various ionic concentrations and species and at higher resolution [19,20]. To date, all of the X-ray structures are missing the first 22 amino acids and the C-terminal domain of ~30 amino acids. A model including the structures of these regions has been generated on the basis of EPR data [21]. As will be discussed below, all of these structures correspond to the *closed* state of the channel. Both computational and EPR-based approaches [22,23] have been used to suggest a model of the open state of KcsA. It is also possible to model an open state of KcsA [24] by comparison with the X-ray structure of a prokaryotic calcium-gated K channel crystallised in its open state [25].

The fold of KcsA (as first revealed in the 3.2 Å structure and confirmed in more recent structures) is shown in Fig. 2A. As predicted by the topological studies, each subunit contains two transmembrane helices (M1 and M2) in between which there is a reentrant P-loop containing the selectivity filter. The P-loop is made up of a descending P-helix and an ascending filter region containing the TVGYG sequence motif which adopts an extended conformation. The filter region is narrow and contains ion-binding sites (see below) formed by rings of backbone oxygen atoms

Table 1
KcsA structures

PDB code	Resolution (Å)	M^+	Comments
1BL8	3.2	K^+	
1J95	2.8	K^+ and TBA	
1JVM	2.8	Rb^+ and TBA	
1K4D	2.3	Low K^+ and Fab	
1K4C	2.0	High K^+ and Fab	
1F6G	EPR	pH 7.2	Full length
1JQ1	EPR	pH 4.0	Open state

TBA = tetrabutylammonium; "full length" is the EPR-derived structure of the complete KcsA molecule, including the N- and C-terminal regions [21]; "open state" is a model of the open conformation of KcsA (M2 helix bundle Cα atoms only) derived from EPR experiments.

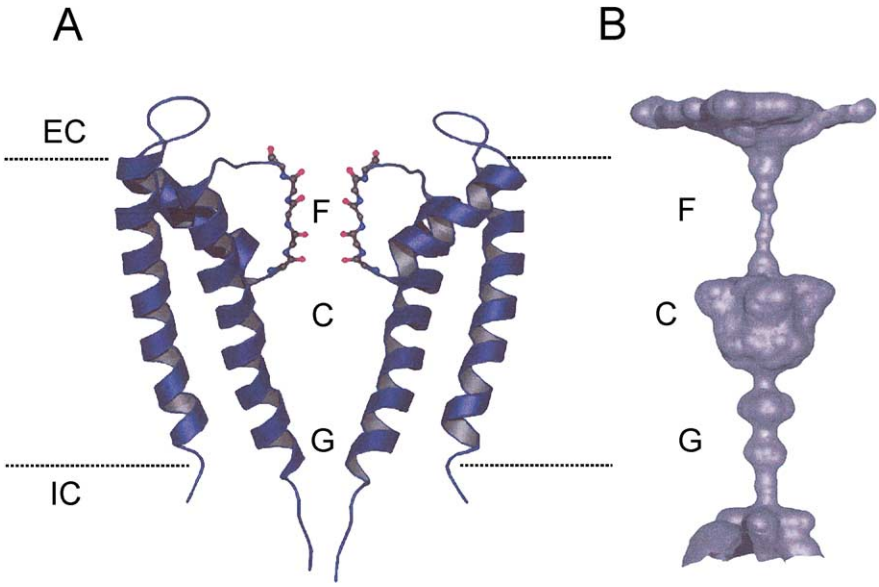

Fig. 2. KcsA fold and pore. (A) Two of the four subunits of KcsA, viewed down a perpendicular to the pore axis. The helices are shown as ribbons; all backbone atoms of the selectivity filter are shown in ball-and-stick format. The lipid bilayer is indicated by the horizontal dotted lines. IC = intracellular; EC = extracellular. (B) The pore-lining surface of KcsA (calculated using HOLE [107,108]) aligned with the fold diagram in (A) and showing the filter (F), cavity (C) and gate (G) regions. Diagrams generated using VMD [109] and Povray.

oriented towards the pore centre. Three key functional regions of the channel can be visualised via the pore-lining surface (Fig. 2B). From this, it can be seen that there are constrictions at both the extracellular and intracellular ends of the channel, with a wider central cavity. The extracellular constriction corresponds to the selectivity filter; the intracellular constriction corresponds to the gate (see below). The water-filled cavity provides an energetically favourable environment for a K^+ ion in the otherwise hydrophobic interior of a membrane [26].

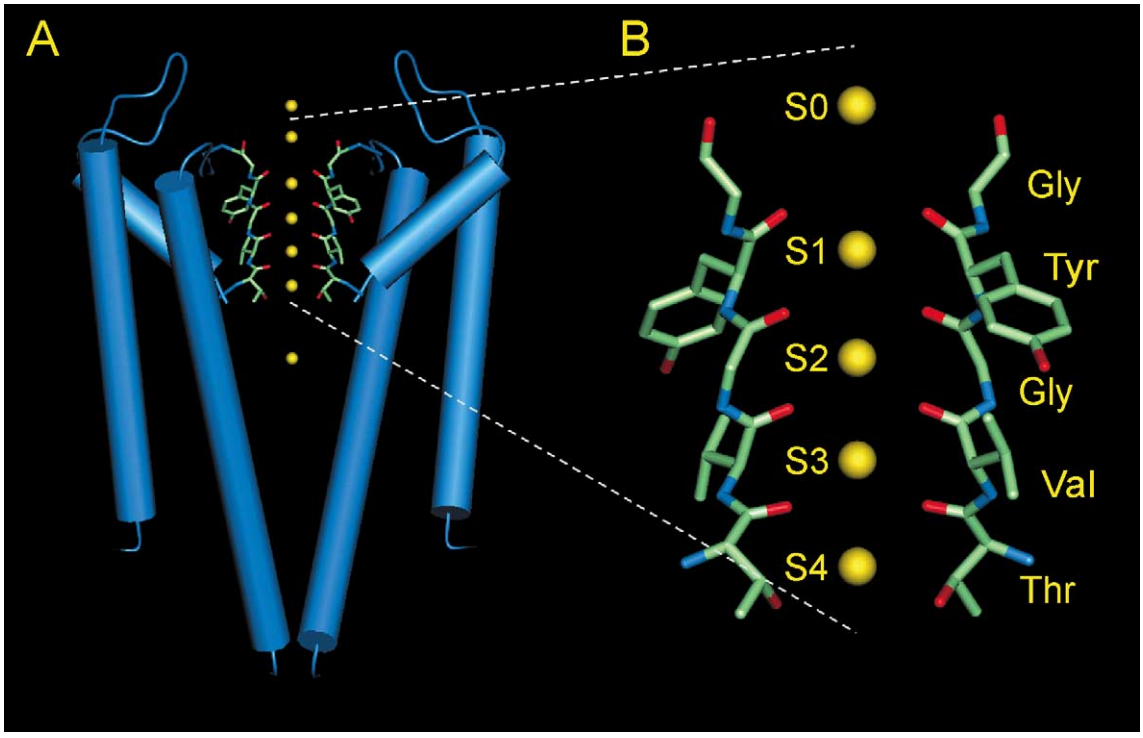

Fig. 3. Structure of KcsA in the presence of high [K^+] (1k4c; [20]). (A) Two subunits of the four are shown (blue), plus the seven locations of K^+ ions revealed in the X-ray structure. These are (from top to bottom): the external mouth, the five sites (S0–S4) in the filter, and the central cavity. (B) A more detailed view of the selectivity filter, again showing two of the four subunits. Ions at sites S0 to S4 are shown.

In the lower (3.2 Å) resolution X-ray structure of KcsA, four ion binding sites within the filter were identified (sites S1 to S4; Fig. 3). It was therefore suggested that ion permeation through the narrow filter region of a K channel required the K^+ ion to be stripped of its hydration shell [18]. Thus, when a K^+ ion is within the filter, its hydration shell is replaced by eight O atoms of the backbone carbonyl groups or (at site S4) four carbonyl O atoms and four hydroxyl O atoms of threonine side chains. The 2.0 Å resolution crystal structure revealed details of both hydration and coordination within the filter (albeit at a temperature of 100 K). The coordination of K^+ ions within the filter at each of the four sites S1 to S4 is made up of eight O atoms from the protein arranged at the corners either of a distorted cube (a square anti-prism) for sites S1 to S3, or of a cube (at site S4), with a K^+ ion at its centre. The higher resolution structure reveals two further K^+ ion sites not observed in the earlier structure, namely S0 and S_{EXT}. S0 is formed by four O atoms (from the carbonyls of G79), with the remaining interactions provided by water molecules. Thus, the K^+ ion's hydration shell has been half-replaced by interactions with the protein. S_{EXT} is on the extracellular side of site S0, and an ion at this site remains surrounded by eight waters. The higher resolution structure also resolves a single K^+ ion within the central cavity, solvated by eight water molecules in a square anti-prism arrangement. Thus, the structures support the suggestion that KcsA (and by extension other K channels) is a multi-ion pore, with a succession of up to six sites in a row in capable of binding K^+ ions (plus a further binding site in the central cavity).

The structure of KcsA crystals in the presence of a low concentration (3 mM) of K^+ ions reveals that there is a degree of flexibility in the selectivity filter. Under such conditions, there are K^+ ions bound mainly at S1 and S4, with some distortion of the polypeptide backbone, especially at residue V76 which contributes to site S3. This conformational change is accompanied by insertion of water molecules between the selectivity filter and the surrounding protein. This result is important in demonstrating that the selectivity filter region is flexible, and that its exact conformation is dependent on the nature of its interactions with bound cations, even within a crystal at low temperatures. Thus, one might anticipate some degree of flexibility in the filter conformation of a K channel protein in a membrane at physiological temperatures.

3. Computational approaches to structure/function relationships

3.1. Permeation

An atomic resolution understanding of the mechanism of ion permeation through K^+ channels is beginning to emerge through integration of physiological, structural and computational results. On the experimental side, by comparing high resolution X-ray structures at low (3 mM) and high (200 mM) K^+, it can be shown that at high K^+ all four sites are (on average) equally occupied [19]. This is consistent with a relatively flat permeation energy landscape and hence with a high permeation rate for K^+ ions. The mechanism of rapid permeation is envisaged in terms of rapid shuttling between two configurations: one with K^+ ions at sites S1 and S3 and another with ions at sites S2 and S4. Approximately equal probabilities of occurrence of these two configurations results in equal *average* occupancies of sites S1 to S4 as observed in the crystal structure. Comparison of K^+ vs. Rb^+ occupancies in the crystal structures has provided further evidence of fine-tuning (via evolution) for K^+ selectivity. In particular, the energy landscape is flatter for K^+ than for Rb^+, and Rb^+ is not seen to occupy site S2 significantly.

These experimental results are mirrored in (and were to some extent predicted by) computer simulations of ion permeation. Guidoni et al. [27] used MD simulations to explore the entry of ions into the filter via the extracellular mouth and confirmed that this required dehydration of the ions and was aided by the electrostatic field created by the protein in that region. Simulations of K^+ ions within the filter [28,29] revealed that two ions plus an intervening water molecule could move in a concerted fashion along the filter, such that K^+ ions were present at either sites S1 and sites S3 or S2 and S4. Free energy calculations comparing different configurations of K^+ ions within the filter [30,31] suggested that the permeation energy landscape is relatively flat, e.g. that the difference in free energy between a configuration with K^+ ion at sites S1 and S3, and a configuration with ions at S2 and S4 is quite small. A number of studies [32,33] have used Brownian dynamics simulations [34] to bridge the gap between the time scale of MD simulations (up to ca. 10 ns) and that of physiological measurements of ion permeation (ca. 1 ms). However, such studies are dependent upon a model of the *open* state of the channel (see below). A number of MD simulations [29,31,35] have revealed local distortions of the filter in response to ion movements, particularly in the region of the valine residue of the TVGYG sequence motif (or the equivalent isoleucine residue of the TIGFG motif in a Kir channel model—see below).

More recent simulation and experimental studies have shown a remarkable convergence. Analysis of a long MD simulation from our laboratory (Fig. 4) and of extensive MD simulations from Benoit Roux's laboratory [31] have revealed that, in addition to sites S1 to S4 within the filter, there is a site S0 at the external mouth of the filter (Fig. 5). This is seen in detail in the high-resolution X-ray structure in the presence of a high K^+ concentration [20], where it can be seen that when present at this site, a K^+ ion interacts with four carbonyl oxygens plus four water molecules. The X-ray structure also suggests an additional more extracellular site (S_{EXT}) at which the ion is surrounded by eight water molecules. It should be remembered that this is at a temper-

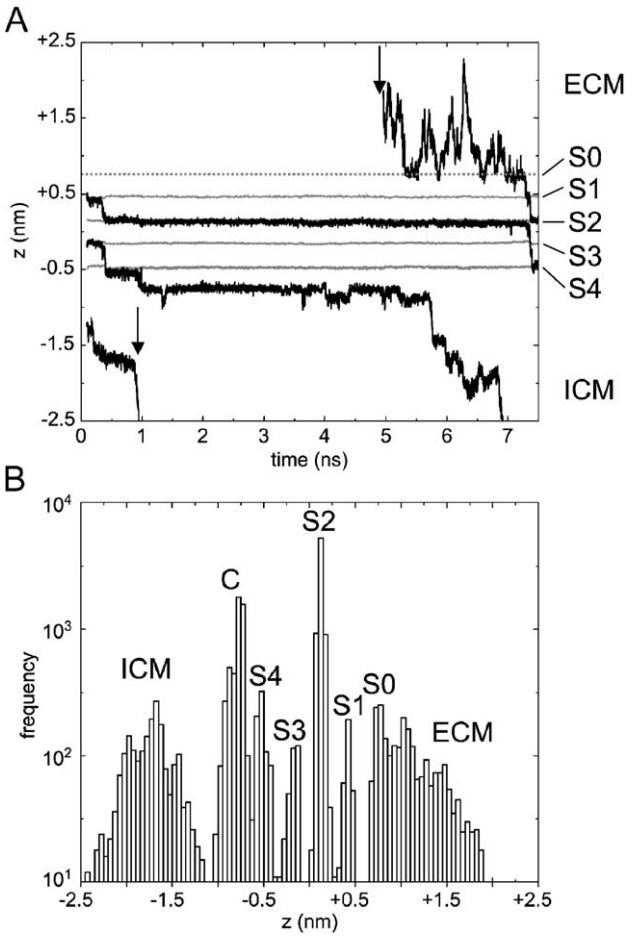

Fig. 4. Simulated movement of K^+ ions through the filter, from a 7 ns MD simulation of KcsA in a POPC bilayer (Shrivastava and Sansom, unpublished data). (A) K^+ ion trajectories projected onto the pore (z) axis, showing the z position of each ion as a function of time. The horizontal grey lines indicate the positions of the centres of sites S0 (dotted line) to S4. The initial configuration of ions in the filter is 01010. There is also a K^+ ion initially in the cavity; at the time indicated by the left-hand arrow, this exits from the pore. The right-hand arrow indicates the same K^+ ion, after exiting the simulation box at negative z and reentering (by virtue of periodic boundary conditions) at positive z. (B) Histogram of K^+ ion positions along the pore (z) axis for the same simulation as in (A). The peaks correspond to distinct 'sites' within the channel, namely S0 to S4, and the cavity (C). ICM and ECM are the intracellular and extracellular mouth regions, respectively.

ature of 100 K; in the simulations (at 300 K), the existence of S_{EXT} as a distinct site is less clear-cut.

From these experimental and computational studies, there emerges a model of the mechanism of permeation. Rapid movement of ions through the filter depends on the relatively flat permeation energy landscape, such that switching between alternative ion configurations occurs at high frequency (see Fig. 6). This is consistent both with the combined physiological and structural studies [19] and with the various simulation studies. Both classes of study also suggest the possibility of states where the filter is occupied by a single K^+ ion, especially at low [K^+]. In addition to the (multiple) ions in the filter, a K^+ ion may also reside within the central cavity. It has been shown that the electrostatic field due to the dipoles of the P-helices can stabilise a K^+ ion in the centre of the cavity [26]. The recent X-ray studies show this ion to be surrounded by a cage of eight water molecules at 100 K; at room temperature, simulations suggest that exact arrangement of the water molecules will be coupled to the location of the ion [36], and also suggest the possibility of interaction with the side chains of a ring of four threonine residues at the far end of the cavity from the filter [28].

However, in trying to complete the picture of permeation, it must be remembered that the X-ray structures of KcsA all correspond to what is almost certainly a *closed* state of the channel. While it does not seem likely that major changes in conformation of the filter region occur during the closed → open transition, movements of the M2 helices have to occur (as suggested by simulations [28,37]) in order for a K^+ ion to enter/leave via the intracellular mouth.

3.2. Selectivity

To what extent do we understand the selectivity mechanism of K channels for K^+ over Na^+ ions? From the initial X-ray structure of KcsA, it was suggested that the main element of selectivity arises from the geometry of the filter, which provides a series of cages of eight oxygen ligands that are optimal placed to interact with a K^+ ion (radius 1.33 Å) and thus compensate fully for the energetic cost of dehydration of K^+ on entering the filter. In contrast, the eight oxygens of each cage cannot interact optimally with the

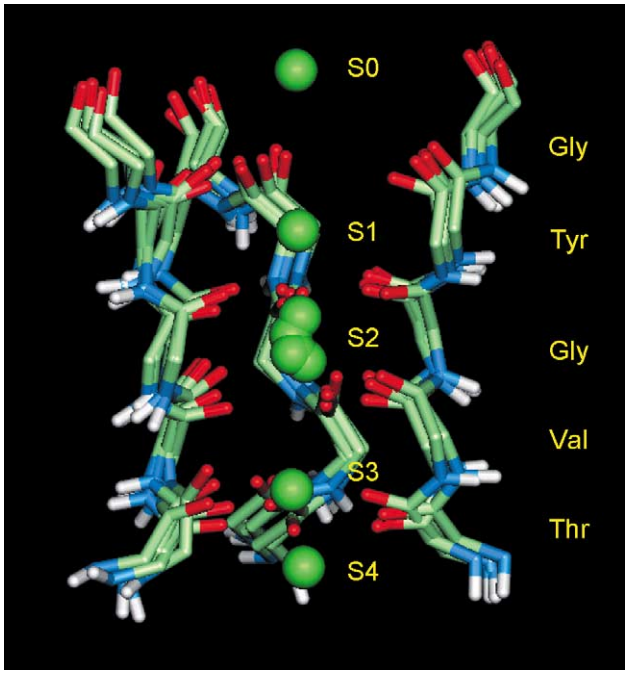

Fig. 5. Potassium ions in the selectivity filter as seen in the same simulation discussed in Fig. 4. Four snapshots from the simulation are superimposed, showing the filter regions of three of the four subunits, and the K^+ ions (green spheres) that occupy (at different times) sites S0 to S4.

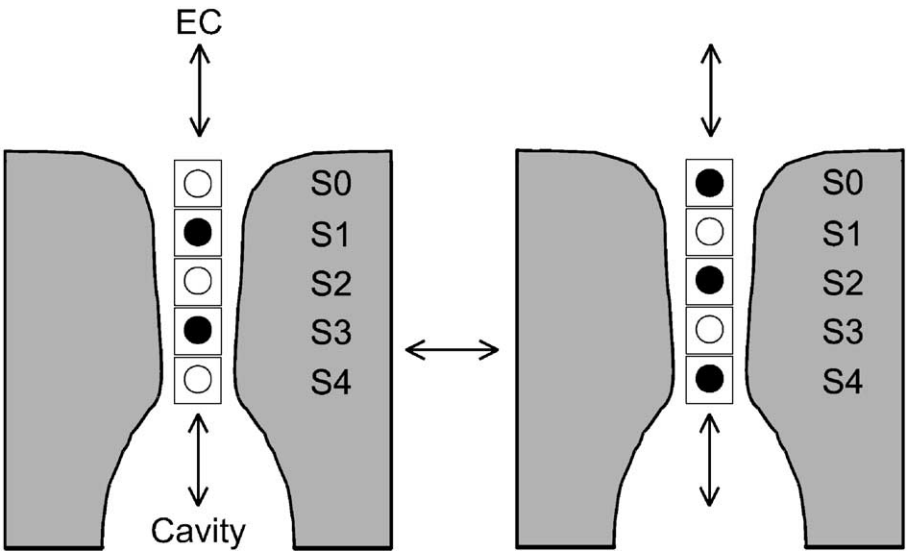

Fig. 6. Schematic diagram of the alternating patterns of occupancy of the selectivity filter by K^+ ions (●) and water molecules (○) that are proposed to underlie rapid permeation of K^+ ions through the KcsA channel. The left-hand configuration would be defined as 01010 and the right-hand configuration as 10101.

smaller (radius 0.95 Å) Na^+ ion, and thus are unable to fully compensate for dehydration. This view is in agreement with energetic calculations based on simulations [30,38,39]. However, as mentioned above, both recent higher resolution structural studies and longer simulations provide evidence for a degree of conformational flexibility in the filter. Thus, one might envisage that the filter could distort to accommodate a Na^+ ion (at some energetic cost). This is seen in simulations where Na^+ ions are placed within the filter of KcsA [35]. Some K channels are known to conduct Na^+ ions, albeit poorly [40,41]. Thus, the question becomes one of comparing the energetics of a filter containing K^+ ions vs. one containing Na^+ ions, taking into account possibly slow distortions of the filter, relative to K^+ vs. Na^+ in bulk solution. This remains a challenge for the future.

3.3. Block

K channels can be blocked both externally (i.e. via interactions at the extracellular mouth) and internally via large positively charged species (blockers). External blockers include tetraethylammonium (TEA) and various peptide toxins; internal blockers include TEA and also the inactivation domain located at the N-terminus of some Kv channels.

Block of K channels by extracellular TEA depends on the presence of an aromatic residue (position 449 in the Shaker potassium channel [42–44]) located near the extracellular mouth of the channel. KcsA can also be blocked by extracellular TEA [11,45] and the affinity of block is influenced by an equivalently positioned residue, Y82. From the structure of KcsA and the location of this tyrosine, one may infer a square-shaped binding site nearly 12 Å across. This is larger than TEA (about 6–8 Å) and therefore has raised concerns about initial interpretations made without the benefit of a crystallographic structure of a KcsA/TEA complex.

Two groups have published simulation studies of the interaction of externally applied TEA with KcsA: Crouzy et al. [46] used MD simulations, while Luzhkov and Åqvist [47] used an automated docking procedure in combination with a method for analyzing binding modes and energies. Both simulation studies agree qualitatively with the experimental observation that TEA binds more strongly to the wildtype (Y82) structure than to KcsA mutants with non-aromatic substitutions at that position. Both groups suggest that the enhanced wildtype complex stability cannot be attributed to π-cation interactions as had been previously postulated. Instead, it is suggested either that the stabilization of TEA binding arises from increased hydrophobic interactions with the aromatic groups forming a cage around the TEA [47] or that the difference in stability between wildtype and Y82T mutant TEA complexes arises from differences in the hydration structure surrounding the TEA molecule [46].

It has been shown previously that a modified version of KcsA with three mutations at its extracellular mouth (Q58A, T61S and R64D) can bind the scorpion toxin Lq2 [8]. Cui et al. [48] have performed Brownian dynamics on this system in order to investigate the nature of the interactions. Their simulations provide additional support for the suggestion [49,50] that toxins in this family exert their effect via a conserved lysine side chain (K27 in Lq2) which acts as a "plug" inserted into the selectivity filter, thereby preventing ion conduction.

The site of external block may be a potential target for drug design. In order to exploit this, a more complete understanding of (long-range) electrostatic interactions between toxins and the channel mouth is required. Such interactions will depend on conformational mobility of both

the channel entrance and the toxin. Recent simulation studies (Tate, Biggin and Sansom, unpublished results) suggest that the electrostatic field surrounding a toxin molecule (Fig. 7) can exhibit substantial fluctuations on a nanosecond time scale. It will be of interest to explore the possible implications of these for the early stages of toxin–protein recognition.

Nearly all potassium channels are also blocked by tetra-alkyl ammonium ions (TEA and homologues) on the *intracellular* side of the channel. A number of studies [51,52] have suggested that the specificity of these blocking agents is governed by the hydrophobicity of the blocker. Luzhkov and Åqvist [47] studied internal block by TEA and found that the binding energies of internal block were very similar to those for external block Structural studies have also provided some insights into internal block [53]. In particular, it seems that there is a binding site for tetra-alkyl ammonium ions within the cavity of the (closed) channel. Further structural and computational studies are needed to explore the nature of internal block in more detail.

3.4. Gating

Gating has for sometime been a more elusive aspect of K channel function from a structural perspective. Early physiological studies by Armstrong [51] demonstrated that the lower (i.e. intracellular) section of a K channel has to be in an open conformation in order to allow blocking ions access to their site of interaction. Reinterpreting these data in the context of the KcsA structure lead to the conclusion that the X-ray structure corresponds to a closed state. A number of more recent studies on various K channel [54–56] also support a conformational change at the inner mouth upon channel gating. This is reinforced by a number of simulation studies that indicate an energetic barrier to ion permeation at the inner mouth of the X-ray structure of KcsA [29,38,57]. This is consistent with the detailed examination of the structure which reveals that the inner mouth is narrower than the Pauling radius of a K^+ ion and is lined by hydrophobic side chains.

This view of channel gating is supported by a series of studies from Perozo et al. [22,58,59] who have used EPR measurements to show that the inner (M2) helices of the potassium channel rotate outwards upon channel opening. The movement of these inner M2 helices can be described approximately by three rigid-body components: (i) a $\sim 8^\circ$ tilt relative to the z-axis towards the membrane normal; (ii) a $\sim 8^\circ$ tilt in the x–y plane away from the permeation path; and (iii) a twist of $\sim 30^\circ$ about the helical axis in the counterclockwise direction when viewed from the extrac-

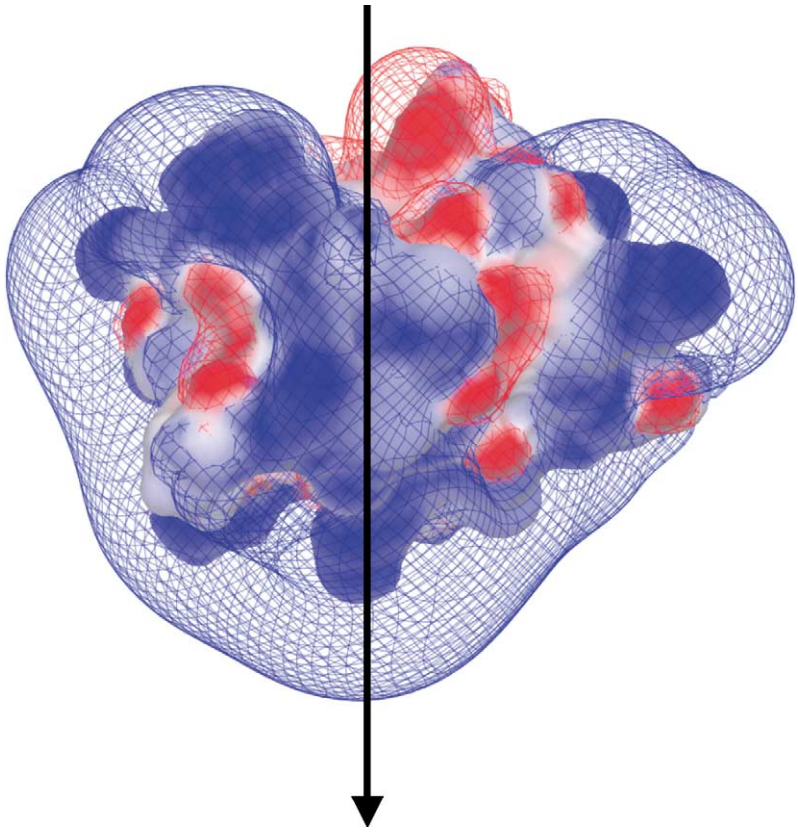

Fig. 7. Structure of Lq2 toxin (pdb code 1LIR) with electrostatic potential contours superimposed. The structure shown is a snapshot from a 3-ns duration MD simulation. The electrostatic potential is contoured at ± 0.6 kcal/mol (i.e. ~ 1 kT) and was calculated for 100 mM salt present. The arrow shows the approximate position of the dipole associated with the toxin molecule, with the K27 residue that is thought to be responsible for binding within the K channel filter at the bottom of the diagram.

ellular side. The data also suggest a semirigid movement involving a slight kinking around residues in the middle of M2 (residues 107–108) that may act as a pivot point. These movements result in an expansion of the intracellular mouth of the channel.

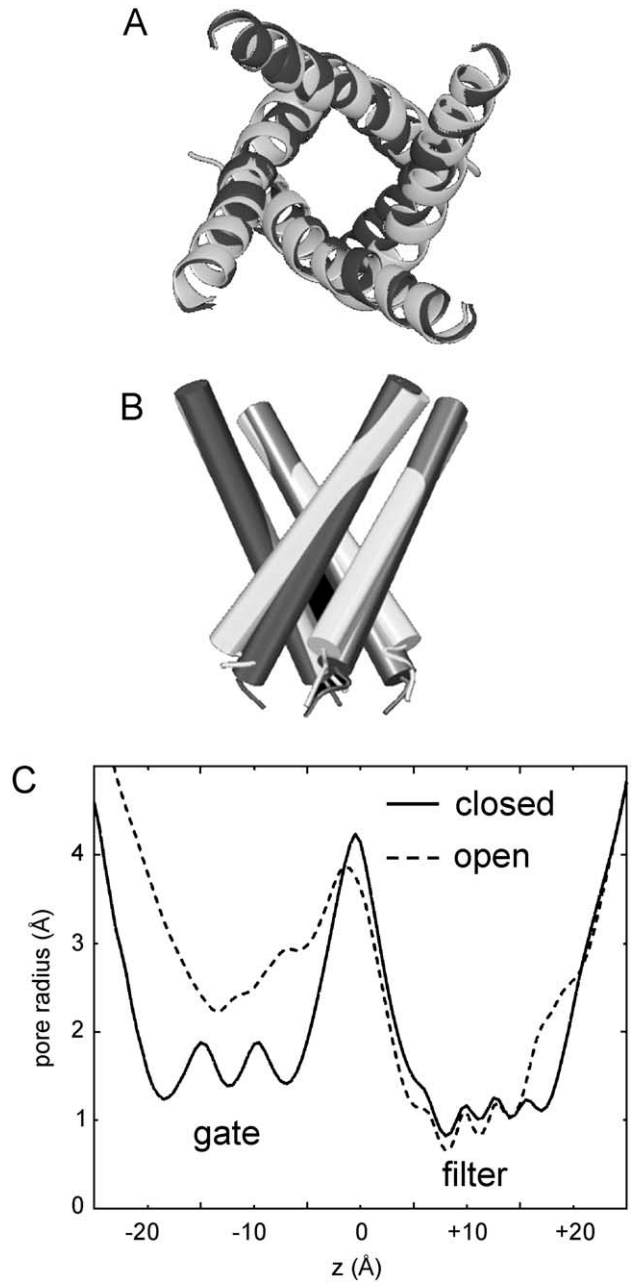

Fig. 8. Modelling the open state of KcsA. The two upper diagrams show a superimposition of the M2 helices from the closed structure (dark grey) and an open state model (light grey) of KcsA. (A) View looking down the pore axis from the filter towards the intracellular mouth of the channel. (B) View down a perpendicular to the pore axis, the extracellular (filter) end of the helices at the top and the intracellular (gate) end of the helices at the bottom. (C) Pore radius profiles for closed (solid line) and open (broken line) state models of the KcsA channel. Both profiles are averages derived from simulations (see Ref. [61] for details).

Mashl et al. [33] have modeled an open state by rotating helices (in particular M2) by $\sim 20^\circ$ in order to produce a channel with a wider radius at the intracellular mouth of the protein. This model has been used in Brownian dynamics simulations of ion permeation. Allen and Chung [60] have also performed BD simulations based on an open state model. In our laboratory, we have attempted to generate open-state models of potassium channels in by steered simulations. One approach to this can be visualised as inflating a van der Waals ''balloon'' inside the channel and observing the response of the protein to this perturbation [61]. The balloon is positioned in the gate region, i.e. the narrow region of the pore at the intracellular mouth. Changes in protein conformation may then be examined to explore a possible transition from a closed to an open state. Structures generated by this procedure show reasonable agreement with the results from models derived by Liu et al. [22] from their data (see Fig. 8). Furthermore, some evidence of hinge-bending of the M2 helices in the vicinity of the G99 residues is seen. Thus, both a purely computational approach [61] and modelling based on restraints from EPR experiments [22,23] lead to a similar picture of KcsA gating whereby the M2 helices move apart in order to open that channel by removal of the narrow hydrophobic barrier at the intracellular mouth. However, the mechanism whereby a lowering of intracellular pH [10,11] leads to such a movement remains unknown. It will also be important to see whether the gates of other families of K channels are located in the same region (see below).

Recently, an X-ray structure has been determined for MthK, a calcium-gated K channel from *Methanobacterium thermoautotrophicum* [25]. Although the resolution of the structure is somewhat limited, especially in the channel domain, it appears that this K channel has been crystallised in an open state. The M2 helices are splayed open relative to those in KcsA. Comparison of the X-ray structures of KcsA (closed) and MthK (open) suggests a gating model in which the M2 helices move approximately radially outwards upon channel activation [24]. The degree of movement of the M2 helices seems to be somewhat greater than that suggested by, e.g. the EPR data. Interestingly, the M2 helices appear to show some hinge-bending in the vicinity of a conserved glycine residue (G99 in KcsA) in the middle of the helix. Such hinge bending close to G99 was also observed in the computational studies of KcsA gating [61]. Thus, a unified model of KcsA gating is starting to emerge.

4. Towards other K channels—homology modelling

Given the sequence similarities (at least in the central pore-forming region) between different K channels, it is important to explore the extent to which a bacterial K channel structure may be used as a template upon which to model the corresponding region of other (mammalian) K

channel families. We will explore two aspects of this, with respect to the Kir and Kv channel families.

4.1. Kir channels

Inwardly rectifying K channels (Kirs) are a family of K channels that conduct K^+ ions from outside to inside the cell more readily than in the opposite direction (a property known as *inward rectification*) [62,63]. They are gated by either G-proteins or ATP. Kirs contain fewer than 500 amino acids per subunit and share the simple 2 TM helix topology with KcsA. However, unlike KcsA, they contain substantial N- and C-terminal domains that are implicated in biological regulation of channel gating. Furthermore, they may interact with other proteins in order to be functionally gated. For example, each Kir6.2 channel is thought to interact with an outer ring of four SUR1 subunits (each containing 17 TM helices) in order to generate a fully functional K_{ATP} channel [6,64].

Although Kirs share a common TM topology with KcsA (i.e. 2 TM helices plus a P-loop per subunit), they are otherwise somewhat distantly related with a sequence identity of only ~15%. Consequently, there has been some debate over whether Kirs have the same architecture for their transmembrane domain as that in KcsA [65,66]. Fundamental to this debate is the problem of obtaining an optimal alignment of Kirs with KcsA, as any homology model will be dependent on this alignment. Alternative alignments of Kir with KcsA (Fig. 9) have been proposed, drawing on structural information from a variety of techniques, including hydropathy analysis, mutagenesis studies, accessibility calculations, and computer simulations of isolated helices (as discussed in Ref. [67]).

On the basis of the different sequence alignments, different various homology models of Kirs have been generated. For example, Thompson et al. [68] constructed models of Kir2.1 using alternative alignments in an attempt to explain the role of three residues that contribute to channel block by Rb^+ and by Cs^+ ions. Loussouarn et al. [69] used the alignment originally proposed in Ref. [18] to show that a KcsA-like structure for another Kir, Kir6.2, was consistent with Cd^{2+} accessibility data following cysteine scanning mutagenesis of the second transmembrane domain. More recently, comparisons [70] of two Kir6.2 models have been performed using MD simulations. One model was KcsA-like, using the same alignment [18] for the M2 region used in previous modelling and simulation studies [67]. In an alternative model, based on the alignment proposed in Ref. [65], residues at the intersubunit interfaces in Kir were identified on the basis of second site suppressor mutation studies and were aligned with residues at the intersubunit interface in the X-ray structure of KcsA. In two long (10 ns) MD simulations, the more KcsA-like model was identified as significantly more structurally stable. This was interpreted as favouring the initial alignment [18] and model [67], and thus indicating that KcsA is indeed a suitable template structure for Kir channels. It is also noteworthy that the initial alignment conserves the glycine residue (G99 in KcsA) that is proposed to play a key role in channel gating (see Section 3.4 above).

The discovery of a family of bacterial homologues of Kirs has helped to shed light on this problem by reducing the ambiguity in alignments of Kirs with KcsA [71]. These bacterial Kir homologue sequences are intermediate in nature between mammalian Kirs and bacterial KcsA. Fig. 9 shows the two alternative alignments of Kirs with KcsA used in comparative modelling and simulation studies [70] along with the alignment of a bacterial Kir with KcsA and mammalian Kirs proposed in Ref. [71]. This alignment supports the use of KcsA-like models of Kirs.

Overall, these studies suggest that homology modelling is a useful way of interpreting experimental information about a channels function. However, only by taking into account all structural information and considerations can we hope to successfully generate a plausible homology model in a case such as this where the sequence identity is so low.

Another way in which to evaluate whether or not a homology model of a membrane protein is reasonable is to examine the transmembrane distribution of residue types and see whether this is consistent with that seen in membrane proteins of known structure [72]. For example, it has

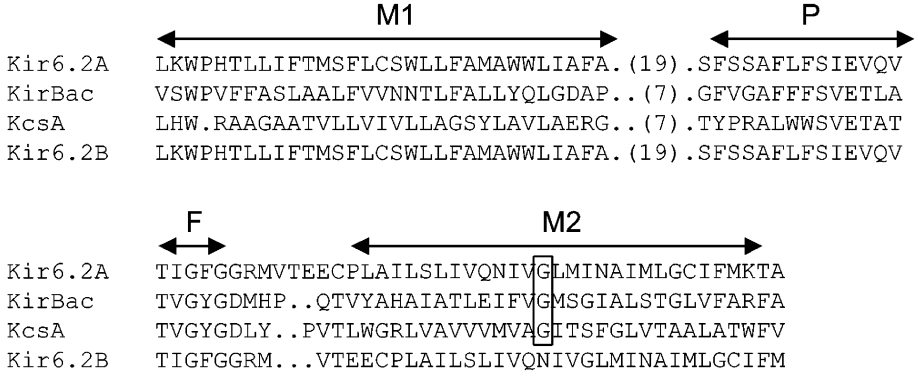

Fig. 9. Inward rectifier K channels. The sequence alignment compares model A and model B of Kir6.2 with KcsA and with a bacterial Kir homologue (KirBac). The M1, P and M2 helices plus the selectivity filter (F) are indicated. The box indicates the glycine (G99 in M2 of KcsA) that is thought to act as a hinge residue in channel gating.

been demonstrated that aromatic side chains, especially tryptophan, tend to be located close to the lipid/water interface [73]. If we examine the locations of aromatic side chains in KcsA and in the preferred homology model [67] of Kir6.2 we see similar distributions, corresponding to the bilayer/water interfacial regions (Fig. 10A,B).

Differences between KcsA and Kir6.2 are seen in the selectivity filter region (Fig. 10C,D). In particular, the tyrosine side chain of the TVGYG sequence motif in KcsA is replaced by a phenylalanine in Kir6.2 (TIGFG). It has been suggested that an H-bond formed by the tyrosine in KcsA plays an important role in maintaining the conformation of the filter at an optimum for K^+ interactions [18]. Such an H-bond is not possible in Kir6.2. In the light of recent results concerning the flexibility of the selectivity filter (see above), it will be of interest to use, e.g. simulations of Kir6.2 [67,74] to explore the implications of the loss of this H-bond in terms of filter flexibility. In particular, it has been suggested that local fluctuations in filter geometry in Kirs may be important with respect to 'fast flicker' gating of these channels [75]. Mutations in the filter region have an effect on Kir channel fast flicker gating [41,76] and simulation studies (Capener and Sansom, unpublished results) suggest that such changes may correlate with changes in local structure of the filter, similar to the changes in KcsA filter conformation seen in the presence of low $[K^+]$.

4.2. Kv channels

Voltage-gated (Kv) channels present a more complex challenge to attempts at modelling. The TM topology of Kv channels includes 6 TM helices per subunit (Fig. 11) plus N-terminal domains and ancillary subunits (see below and Table 2). Here we focus on the core pore-forming domain (S5-P-S6 in Kv, homologous to M1-P-M2 in KcsA). There is significant sequence identity (ca. 30%) between KcsA and Kv in this region, and a number of experimental studies have demonstrated structural and functional similarities [8,77]. On this basis, it has been possible to generate homology models of the core pore-forming region of, e.g. Shaker Kv channels [78] in attempts to understand permeation, block [79] and gating [80] in such channels.

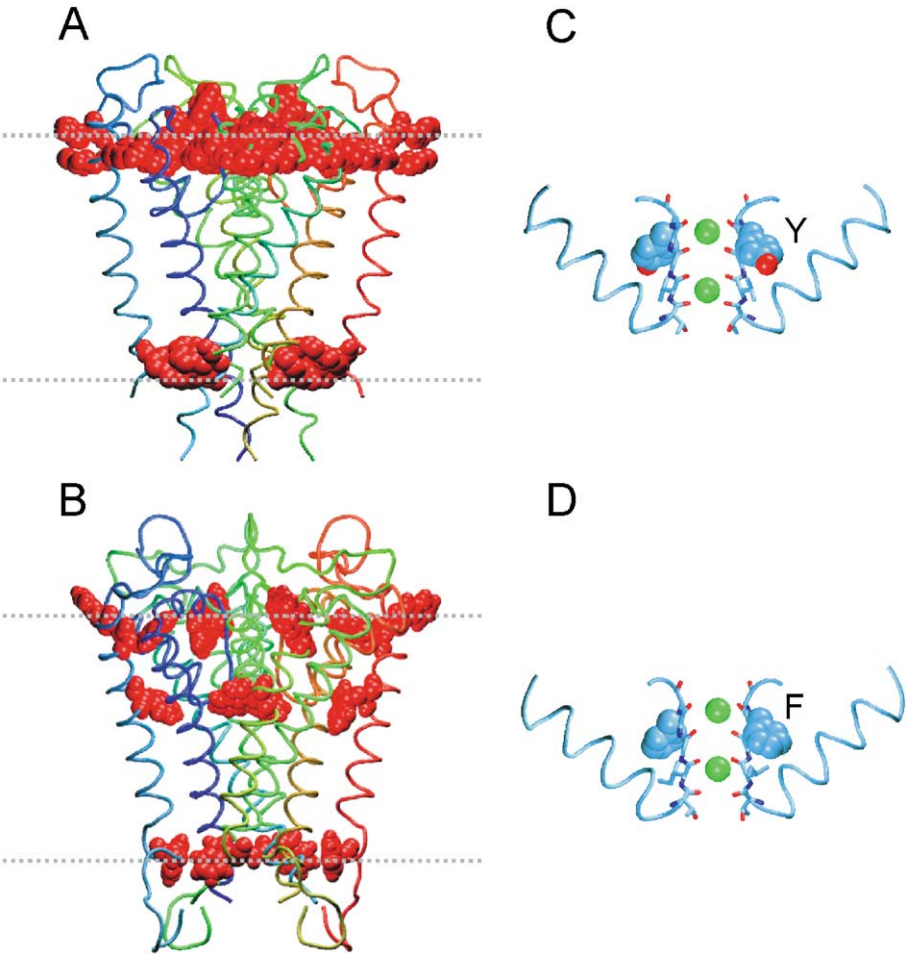

Fig. 10. Comparison of the structures of KcsA and Kir6.2 transmembrane domains. The KcsA (A) and Kir6.2 model (B) tetramers are shown with tryptophan and tyrosine side chains in space-filling format (red). The broken grey lines indicate the approximate position of the lipid bilayer. The filter regions plus P helices of KcsA (C) and Kir6.2 (D) are compared, with K^+ ions at sites S1 and S3. The tyrosine (Y) and phenylalanine (F) of the selectivity filters of KcsA and Kir6.2, respectively, are shown in space-filling format and are labelled.

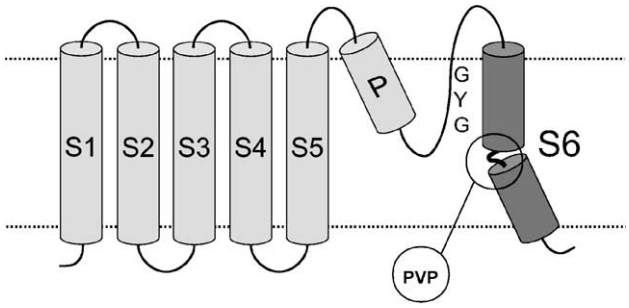

Fig. 11. Transmembrane topology of a Kv channel subunit. The S6 helix (dark grey) is shown as kinked in the vicinity of its PVP 'hinge' (circled).

However, there is a complication in that the S6 helix of Kv channels (which corresponds to the M2 helix of KcsA) contains a conserved Pro-Val-Pro motif (Fig. 11). Modelling and simulation studies on isolated S6 helix models in a membrane-like environment [81–83] suggest that: (i) the S6 is kinked in the vicinity of the PVP sequence motif; and (ii) the local distortion of the helix in the vicinity of the PVP motif may be able to act as a hinge, enabling dynamic changes in helix conformation (Fig. 12A). Although it is evident that the flexibility of S6 may be restricted once it is incorporated in a model of a complete Kv channel (or even of a tetramer of the S5-P-S6 bundle), it seems likely that even in the intact channel, S6 remains kinked (Fig. 12B). The latter is supported by experimental evidence from Yellen et al. [84,85] who have used cysteine-scanning plus chemical modification to explore the conformation of S6 in Shaker Kv channels. Mutations in the vicinity of the Pro-Val-Pro motif alter the voltage-sensitivity of activation of Kv channels [86–88], suggesting that local changes in conformation about the dynamic hinge may be involved in the gating mechanism of the channel.

Concerning the remainder of the protein (e.g. the outer 'rings' of S1 to S4 helices), there is relatively little unambiguous structural information. NMR studies on isolated TM segments have established that, e.g. S4 is α-helical in membrane-like environments [89]. Systematic fluorescence scanning studies have been used to probe the structural dynamics of Kv channels, with an overall aim of characterising the local rearrangements in the vicinity of the S4 voltage sensor that accompany channel activation [90,91]. A low (25 Å) resolution structure of the intact Shaker Kv tetramer has been determined [92]. This should provide useful constraints on attempts to model [93] how the various structural elements (including, e.g. T1; see below) in Kv channels are packed together.

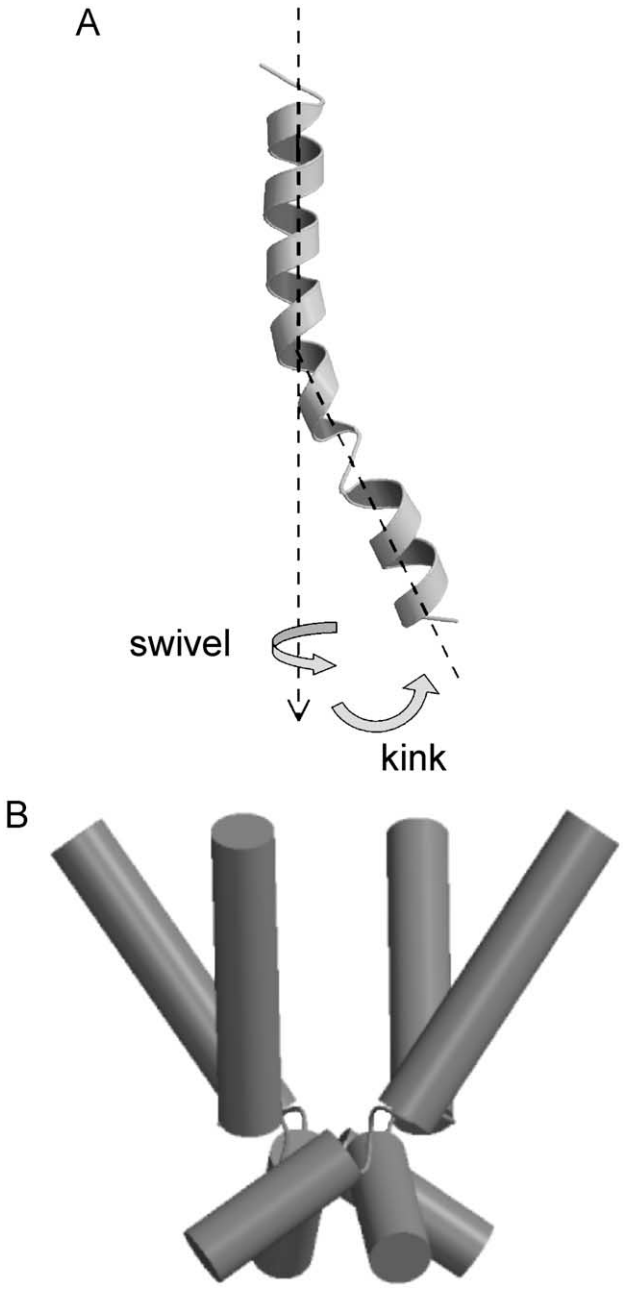

Fig. 12. (A) S6 helix structure taken from a simulation of the isolated helix in a membrane mimetic octane slab [110]. The N-terminus of the helix is at the top of the diagram. The definitions of helix kink and swivel angles are indicated. (B) Schematic model of the inner helix bundle of Kv channel pore as formed by four kinked S6 helices.

Table 2
Ancillary domains and subunits

Domain	Location	Fold	Function	PDB code
Inactivation domain ("ball") peptide	N-terminus	–	Blocks of intracellular ion conduction pathway	1ZTN, 1ZTO
T1 (NTD)	N-terminus	Novel fold	Heterotetramerization and assembly of channels	1A68
Kv β	Separate chain	α/β fold	Regulation	1ID1
CaMBD	C-terminus	Helix–loop–helix	Regulation via Ca^{2+}	1G4Y
MthK RCK	C-terminus	α/β fold	Regulation via Ca^{2+}	1LNQ

5. Structures of ancillary domains/proteins

The architecture of the core pore-forming transmembrane domain is likely to be conserved across all families of K-channels. However, different potassium channels have different physiological roles in cells, and their properties are often regulated by interaction with extramembraneous domains and/or subunits. There have been significant efforts recently in determining the structures of such components. It is perhaps proving a little more difficult to establish their modes of interaction with the transmembrane domain.

Some of the first ancillary domains to have their structures elucidated (e.g. the inactivation domain [94,95], the T1 domain [96–98] and the Kvâ protein [99–101]) have been reviewed in detail recently [13,55,102]. More recent structures include RCK [103] and calcium-sensing [104] domains (see below). A summary of structures is provided in Table 2.

5.1. The RCK domain

In calcium-sensitive large conductance K-channels, there is a regulatory domain C-terminal to the pore-forming TM domain. This domain is known as an RCK domain (regulates conductance of K^+) and exhibits a Rossman fold. Its position in the sequence (i.e. just after the inner helices of the pore) means that it is ideally positioned to exert control over the conduction of ions through the pore. RCK domains are found not only in eukaryotic BK channels, but also in many prokaryotic K channels and in prokaryotic transport system subunits such as TrkA [105]. A number of these domains include a glycine motif (GXGXXG. . .D) that may indicate a role for NAD binding. It remains to be seen how such domains are organized with respect to the bilayer and how they are coupled to conformational transitions of the pore domain. However, a clue is provided by the X-ray structure of a bacterial Ca-gated K channel MtkH (see above) [25]. This has revealed the structure of an octameric assembly of a Ca-binding RCK domain attached to the cytoplasmic mouth of the channel via a flexible linker peptide from the C-terminus of the transmembrane M2 helix. It is suggested that Ca-binding leads to a change in RCK domain/domain interactions that in turn pulls the M2 helices outwards so as to open the channel, although such direct mechanism is perhaps difficult to reconcile with the apparently flexible linker region.

5.2. The calcium-sensing domain

Further "downstream" in the sequence of (eukaryotic) Ca-gated K channels, calcium-sensing domains are found. Small conductance Ca^{2+} activated K^+ channels (SK channels) are gated solely by Ca^{2+} and are not sensitive to voltage. These channels bind calmodulin (CaM) via a calmodulin-binding domain (CaMBD). The CaMBD has a simple fold consisting of two long α-helices connected by a loop. The channel opens when Ca^{2+} binds to the EF hands in the N-lobe of the CaM. The structure of a CaMBD/CaM complex has been solved by X-ray crystallography to 1.6 Å resolution [104], revealing CaMBD to be dimeric with CaM bound to both ends such that one CaM is bound to both CaMBD subunits. Interestingly, the CaMBD contains no identifiable CaM interaction motif. Furthermore, the complex is distinct from any other CaM/peptide complex so far observed in that the CaM binds three helices instead of one. Interested readers are referred to Ref. [106] for a more detailed overview of this domain.

6. What next?

Although there have been considerable advances in understanding structure and function of K channels, much remains to be done. From a purely structural perspective, the major challenge lies in determining high-resolution structures of a wider range of (mammalian) K channel families, including those such as Kv channels, with more complex TM and extramembrane domain organisations. From a computational perspective, the major challenges are to improve both fine-grained studies of, e.g. mechanisms of ion selectivity, and also to extend methods to longer time- and length-scale transitions such as channel gating. By integrating these two approaches, we should be able to arrive at a genuinely atomic resolution understanding of how K channels work.

Acknowledgements

Our thanks to many colleagues for discussions concerning K channels, especially Frances Ashcroft, Declan Doyle, and Peter Proks. Work in MSPS's laboratory is supported by grants from the Wellcome Trust. CEC is a BBSRC funded research student.

References

[1] B. Hille, Ionic Channels of Excitable Membranes, 3rd ed., Sinauer Associates, Sunderland, MA, 2001.
[2] R. MacKinnon, Curr. Opin. Neurobiol. 1 (1991) 14–19.
[3] C. Miller, Science 252 (1991) 1092–1096.
[4] O. Pongs, J. Membr. Biol. 136 (1993) 1–8.
[5] Q. Lü, C. Miller, Science 268 (1995) 304–307.
[6] F.M. Ashcroft, Ion Channels and Disease, Academic Press, San Diego, 2000.
[7] H. Schrempf, O. Schmidt, R. Kummerlein, S. Hinnah, D. Muller, M. Betzler, T. Steinkamp, R. Wagner, EMBO J. 14 (1995) 5170–5178.
[8] R. MacKinnon, S.L. Cohen, A. Kuo, A. Lee, B.T. Chait, Science 280 (1998) 106–109.
[9] M. LeMasurier, L. Heginbotham, C. Miller, J. Gen. Physiol. 118 (2001) 303–313.

[10] L.G. Cuello, J.G. Romero, D.M. Cortes, E. Perozo, Biochemistry 37 (1998) 3229–3236.
[11] L. Heginbotham, M. LeMasurier, L. Kolmakova-Partensky, C. Miller, J. Gen. Physiol. 114 (1999) 551–559.
[12] G. Yellen, Curr. Opin. Neurobiol. 9 (1999) 267–273.
[13] P.C. Biggin, T. Roosild, S. Choe, Curr. Opin. Struct. Biol. 10 (2000) 456–461.
[14] D.L. Minor, Curr. Opin. Struct. Biol. 11 (2001) 408–414.
[15] M.S.P. Sansom, I.H. Shrivastava, K.M. Ranatunga, G.R. Smith, Trends Biochem. Sci. 25 (2000) 368–374.
[16] B. Roux, S. Bernèche, W. Im, Biochemistry 39 (2000) 13295–13306.
[17] D.P. Tieleman, P.C. Biggin, G.R. Smith, M.S.P. Sansom, Q. Rev. Biophys. 34 (2001) 473–561.
[18] D.A. Doyle, J.M. Cabral, R.A. Pfuetzner, A. Kuo, J.M. Gulbis, S.L. Cohen, B.T. Cahit, R. MacKinnon, Science 280 (1998) 69–77.
[19] J.H. Morais-Cabral, Y. Zhou, R. MacKinnon, Nature 414 (2001) 37–42.
[20] Y. Zhou, J.H. Morais-Cabral, A. Kaufman, R. MacKinnon, Nature 414 (2001) 43–48.
[21] D.M. Cortes, L.G. Cuello, E. Perozo, J. Gen. Physiol. 117 (2001) 165–180.
[22] Y. Liu, P. Sompornpisut, E. Perozo, Nat. Struct. Biol. 8 (2001) 883–887.
[23] P. Sompornpisut, Y.S. Liu, E. Perozo, Biophys. J. 81 (2001) 2530–2546.
[24] Y. Jiang, A. Lee, J. Chen, M. Cadene, B.T. Chait, R. MacKinnon, Nature 417 (2002) 523–526.
[25] Y. Jiang, A. Lee, J. Chen, M. Cadene, B.T. Chait, R. MacKinnon, Nature 417 (2002) 515–522.
[26] B. Roux, R. MacKinnon, Science 285 (1999) 100–102.
[27] L. Guidoni, V. Torre, P. Carloni, Biochemistry 38 (1999) 8599–8604.
[28] I.H. Shrivastava, M.S.P. Sansom, Biophys. J. 78 (2000) 557–570.
[29] S. Bernèche, B. Roux, Biophys. J. 78 (2000) 2900–2917.
[30] J. Åqvist, V. Luzhkov, Nature 404 (2000) 881–884.
[31] S. Bernèche, B. Roux, Nature 414 (2001) 73–77.
[32] S.H. Chung, T.W. Allen, M. Hoyles, S. Kuyucak, Biophys. J. 77 (1999) 2517–2533.
[33] R.J. Mashl, Y.Z. Tang, J. Schnitzer, E. Jakobsson, Biophys. J. 81 (2001) 2473–2483.
[34] W. Im, S. Seefeld, B. Roux, Biophys. J. 79 (2000) 788–801.
[35] I.H. Shrivastava, D.P. Tieleman, P.C. Biggin, M.S.P. Sansom, Biophys. J. 83 (2002) 633–645.
[36] L. Guidoni, V. Torre, P. Carloni, FEBS Lett. 477 (2000) 37–42.
[37] I.H. Shrivastava, M.S.P. Sansom, Eur. Biophys. J. 31 (2002) 207–216.
[38] T.W. Allen, S. Kuyucak, S.H. Chung, Biophys. J. 77 (1999) 2502–2516.
[39] T.W. Allen, A. Bliznyuk, A.P. Rendell, S. Kuyucak, S.H. Chung, J. Chem. Phys. 112 (2000) 8191–8204.
[40] L. Heginbotham, Z. Lu, T. Abramsom, R. MacKinnon, Biophys. J. 66 (1994) 1061–1067.
[41] P. Proks, C.E. Capener, P. Jones, F. Ashcroft, J. Gen. Physiol. 118 (2001) 341–353.
[42] R. MacKinnon, G. Yellen, Science 250 (1990) 276–279.
[43] L. Heginbotham, R. MacKinnon, Neuron 8 (1992) 483–491.
[44] M.P. Kavanaugh, R.S. Hurst, J. Yakel, M.D. Varnum, J.P. Adelman, R.A. North, Neuron 8 (1992) 493–497.
[45] D. Meuser, H. Splitt, R. Wagner, H. Schrempf, FEBS Lett. 462 (1999) 447–452.
[46] S. Crouzy, S. Berneche, B. Roux, J. Gen. Physiol. 118 (2001) 207–217.
[47] V.B. Luzhkov, J. Åqvist, FEBS Lett. 495 (2001) 191–196.
[48] M. Cui, J.H. Shen, J.M. Briggs, X.M. Luo, X.J. Tan, H.L. Jiang, K.X. Chen, R.Y. Ji, Biophys. J. 80 (2001) 1659–1669.
[49] S.A.N. Goldstein, D.J. Pheasant, C. Miller, Neuron 12 (1994) 1377–1388.
[50] C. Miller, Neuron 15 (1995) 5–10.
[51] C.M. Armstrong, J. Gen. Physiol. 58 (1971) 413–437.
[52] R.J. French, J.J. Shoukimas, Biophys. J. 34 (1981) 271–291.
[53] M. Zhou, J.H. Morais-Cabral, S. Mann, R. MacKinnon, Nature 411 (2001) 657–661.
[54] Y. Liu, M. Holmgren, M.E. Jurman, G. Yellen, Neuron 19 (1997) 175–184.
[55] B.A. Yi, D.L.J. Minor, Y.F. Lin, Y.N. Jan, L.Y. Jan, Proc. Natl. Acad. Sci. 98 (2001) 11016–11023.
[56] R. Sadja, K. Smadja, N. Alagem, E. Reuveny, Neuron 29 (2001) 669–680.
[57] P.C. Biggin, G.R. Smith, I.H. Shrivastava, S. Choe, M.S.P. Sansom, Biochim. Biophys. Acta 1510 (2001) 1–9.
[58] E. Perozo, D.M. Cortes, L.G. Cuello, Nat. Struct. Biol. 5 (1998) 459–469.
[59] E. Perozo, D.M. Cortes, L.G. Cuello, Science 285 (1999) 73–78.
[60] T.W. Allen, S.H. Chung, Biochim. Biophys. Acta 1515 (2001) 83–91.
[61] P.C. Biggin, M.S.P. Sansom, Biophys. J. 83 (2002) (in press).
[62] C.A. Doupnik, N. Davidson, H.A. Lester, Curr. Opin. Neurobiol. 5 (1995) 268–277.
[63] F. Reimann, F.M. Ashcroft, Curr. Opin. Cell Biol. 11 (1999) 503–508.
[64] B. Liss, B. Roeper, Membr. Mol. Biol. 18 (2001) 117–127.
[65] D.L. Minor, S.J. Masseling, Y.N. Jan, L.Y. Jan, Cell 96 (1999) 879–891.
[66] Y. Kubo, Y. Murata, J. Physiol. 531 (2001) 645–660.
[67] C.E. Capener, I.H. Shrivastava, K.M. Ranatunga, L.R. Forrest, G.R. Smith, M.S.P. Sansom, Biophys. J. 78 (2000) 2929–2942.
[68] G.A. Thompson, M.L. Leyland, I. Ashmole, M.J. Sutcliffe, P.R. Stanfield, J. Physiol. 526 (2000) 231–240.
[69] G. Loussouarn, E.N. Amkhina, C.G. Nichols, Biophys. J. 76 (1999) A75.
[70] C.E. Capener, H.J. Kim, T. Arinaminpathy, M.S.P. Sansom, Hum. Mol. Genet. (2002) (in press).
[71] S.R. Durell, H.R. Guy, BioMed Cent. 1 (2001) 14.
[72] M.B. Ulmschneider, M.S.P. Sansom, Biochim. Biophys. Acta 1512 (2001) 1–14.
[73] W.M. Yau, W.C. Wimley, K. Gawrisch, S.H. White, Biochemistry 37 (1998) 14713–14718.
[74] C.E. Capener, M.S.P. Sansom, J. Phys. Chem., B 106 (2002) 4542–4551.
[75] G. Yellen, Nat. Struct. Biol. 8 (2001) 1011–1013.
[76] T. Lu, A.Y. Ting, J. Mainland, L.Y. Jan, P.G. Schultz, J. Yang, Nat. Neurosci. 4 (2001) 239–246.
[77] Z. Lu, A.M. Klem, Y. Ramu, Nature 413 (2001) 809–813.
[78] K.M. Ranatunga, R.D. Law, G.R. Smith, M.S.P. Sansom, Eur. Biophys. J. 30 (2001) 295–303.
[79] A. Wrisch, S. Grissmer, J. Biol. Chem. 275 (2000) 39345–39353.
[80] F. Espinosa, R. Fleischhauer, A. McMahon, R.H. Joho, J. Gen. Physiol. 118 (2001) 157–169.
[81] I.D. Kerr, H.S. Son, R. Sankararamakrishnan, M.S.P. Sansom, Biopolymers 39 (1996) 503–515.
[82] I.H. Shrivastava, C. Capener, L.R. Forrest, M.S.P. Sansom, Biophys. J. 78 (2000) 79–92.
[83] D.P. Tieleman, I.H. Shrivastava, M.B. Ulmschneider, M.S.P. Sansom, Proteins: Struct. Funct. Genet. 44 (2001) 63–72.
[84] D.D. Camino, M. Holmgren, Y. Liu, G. Yellen, Nature 403 (2000) 321–325.
[85] D.D. Camino, G. Yellen, Neuron 32 (2001) 649–656.
[86] D.H. Hackos, K.J. Swartz, Biophys. J. 78 (2000) 398A.
[87] D.H. Hackos, K.J. Swartz, Biophys. J. 80 (2001) 705.
[88] A.J. Labro, A.L. Raes, N. Ottschytsch, D.J. Snyders, Biophys. J. 80 (2001) 1875.
[89] A. Halsall, C.E. Dempsey, J. Mol. Biol. 293 (1999) 901–915.
[90] F. Bezanilla, Physiol. Rev. 80 (2000) 555–592.
[91] C.S. Gandhi, E. Loots, E.Y. Isacoff, Neuron 27 (2000) 585–595.
[92] O. Sokolova, L. Kolmakova-Partensky, N. Grigorieff, Structure 9 (2001) 215–220.

[93] S.R. Durell, Y.L. Hao, H.R. Guy, J. Struct. Biol. 121 (1998) 263–284.
[94] C. Antz, M. Geyer, B. Fakler, M.K. Schott, H.R. Guy, R. Frank, J.P. Ruppersberg, H.R. Kalbitzer, Nature 385 (1997) 272–275.
[95] C. Antz, T. Bauer, H. Kalbacher, R. Frank, M. Covarrubias, H.R. Kalbitzer, J.P. Ruppersberg, T. Baukrowitz, B. Fakler, Nat. Struct. Biol. 6 (1999) 146–150.
[96] N.V. Shen, P.J. Pfaffinger, Neuron 14 (1995) 625–633.
[97] A. Kreusch, P.J. Pfaffinger, C.F. Stevens, S. Choe, Nature 392 (1998) 945–948.
[98] J. Xu, W. Yu, Y.N. Jan, L.Y. Jan, M. Li, J. Biol. Chem. 270 (1995) 24761–24768.
[99] J. Rettig, S.H. Heinemann, F. Wunder, C. Lorra, D.N. Parcej, J.O. Dolly, O. Pongs, Nature 369 (1994) 289–294.
[100] J. Gulbis, S. Mann, R. MacKinnon, Cell 97 (1999) 943–952.
[101] J.M. Gulbis, M. Zhou, S. Mann, R. MacKinnon, Science 289 (2000) 123–127.
[102] R.H. Scannevin, J.S. Trimmer, Biochem. Biophys. Res. Commun. 232 (1997) 585–589.
[103] Y.X. Jiang, A. Pico, M. Cadene, B.T. Chait, R. MacKinnon, Neuron 29 (2001) 593–601.
[104] M.A. Schumacher, A.F. Rivard, H.P. Bachinger, J.P. Adelman, Nature 410 (2001) 1120–1124.
[105] S.R. Durell, Y.L. Hao, T. Nakamura, E.P. Bakker, H.R. Guy, Biophys. J. 77 (1999) 775–788.
[106] G. Yellen, Trends Pharmacol. Sci. 22 (2001) 439–441.
[107] O.S. Smart, J.M. Goodfellow, B.A. Wallace, Biophys. J. 65 (1993) 2455–2460.
[108] O.S. Smart, J.G. Neduvelil, X. Wang, B.A. Wallace, M.S.P. Sansom, J. Mol. Graph. 14 (1996) 354–360.
[109] W. Humphrey, A. Dalke, K. Schulten, J. Mol. Graph. 14 (1996) 33–38.
[110] J.N. Bright, I.H. Shrivastava, F.S. Cordes, M.S.P. Sansom, Biopolymers 64 (2002) 303–313.